Interactions of Metal Ions with Water: Ab Initio Molecular Orbital Studies of Structure, Vibrational Frequencies, Charge Distributions, Bonding Enthalpies, and Deprotonation Enthalpies. 2. Monohydroxides

Mendel Trachtman

Department of Chemistry, Philadelphia University, Henry Avenue and School House Lane, Philadelphia, Pennsylvania 19144

George D. Markham, Jenny P. Glusker,* and Philip George

The Institute for Cancer Research, Fox Chase Cancer Center, 7701 Burholme Avenue, Philadelphia, Pennsylvania 19111

Charles W. Bock

Department of Chemistry, Philadelphia University, Henry Avenue and School House Lane, Philadelphia, Pennsylvania 19144 and The Institute for Cancer Research, Fox Chase Cancer Center, 7701 Burholme Avenue, Philadelphia, Pennsylvania 19111

Received January 3, 2001

The formation and properties of a wide range of metal ion monohydroxides, $M^{n+}[OH^-]$, where $n = 1$ and 2, have been studied by ab initio molecular orbital calculations at the MP2(FULL)/6-311++G**//MP2(FULL)/6-311++G** and CCSD(T)(FULL)/6-311++G**//MP2(FULL)/6-311++G** computational levels. The ions M^{n+} are from groups 1A, 2A, 3A, and 4A in the second, third, and fourth periods of the Periodic Table and from the first transition series. Geometrical parameters, vibrational frequencies, atomic charge distributions, orbital occupancies, and bonding enthalpies are reported. The $M^{n+}-O$ distances are shorter in the hydroxides than in the corresponding hydrates (published previously as Part 1, *Inorg. Chem.* **1998**, *37*, 4421−4431) due to a greater electrostatic interaction in the hydroxides. The natural bond orbitals for most of the first-row transition metal ion hydroxides do not contain a formal metal−oxygen bonding orbital; nevertheless the atomic charge distributions show that for both $n = 1$ and 2 a significant amount of electron density is consistently transferred from the hydroxide ion to the bound metal ion. Deprotonation enthalpies for the hydrates have been evaluated according to the simple dissociation process, $M^{n+}[OH_2] \rightarrow M^{n+}[OH^-] + H^+$, and also via proton transfer to another water molecule, $M^{n+}[OH_2] + H_2O \rightarrow M^{n+}[OH^-] + H_3O^+$. The drastic reduction in these deprotonation enthalpies as H_2O molecules are sequentially bonded in the first coordination shell of the metal ion (amounting to 71, 64, 85, and 91 kcal/mol for the bonding of six water molecules to Mg^{2+}, Ca^{2+}, Mn^{2+}, and Zn^{2+}, respectively) is found to be due to the greater decrease in the bonding enthalpies for the hydroxides relative to the hydrates. Proton transfer to bases other than water, for example side chain groups of certain amino acids, could more than offset the decrease in deprotonation energy due to the filling of the first coordination shell. Linear relationships have been found between the pK_a values for ionization of the Mg^{2+}, Ca^{2+}, Mn^{2+}, Fe^{2+}, Co^{2+}, Ni^{2+}, Cu^{2+}, and Zn^{2+} aquo ions, and ΔH°_{298} for the bonding of the first water molecule, for the bonding of the hydroxide ion, and for proton dissociation from the monohydrate. Similar relationships have also been found between the pK_a values and the reciprocal of the M−O bond lengths in both the monohydrates and hydroxides. Thus the ionization of metal hydrates in water echoes the properties of the monomeric species $M^{n+}[OH_2]$.

Introduction

Metal cations interact with neutral ligands, such as water, in a wide variety of physical, chemical, and biological phenomena.[1] For example, many proteins require a metal ion for function,[2] and many of these protein-bound metal ions are bonded to at least one water molecule.[3] In several metalloenzyme systems the catalytic activity involves deprotonation of a metal ion-bonded water molecule to give a hydroxyl group, still bound to the metal ion. This hydroxy group can then act as a nucleophile and attack the substrate.[4]

* To whom correspondence should be addressed.

(1) Fraústo da Silva, J. J. R.; Williams, R. J. P. *The Biological Chemistry of the Elements*; Clarendon Press: Oxford, U.K., 1991.

(2) Tainer, J. A.; Roberts, V. A.; Getzoff, E. D. *Curr. Opin. Biotechnol.* **1991**, *2*, 582−590.

(3) Katz, A. K.; Glusker, J. P.; Beebe, S. A.; Bock, C. W. *J. Am. Chem. Soc.* **1996**, *118*, 5752−5763.

(4) Whitlow, M.; Howard, A. J. *Trans. Am. Crystallogr. Assoc.* **1991**, 25−126.

10.1021/ic010008p CCC: $20.00
Published on Web 07/13/2001

Deprotonation of the metal ion-hydrate can be represented as *proton dissociation*:

$$M^{n+}[OH_2] \rightarrow M^{n+}[OH^-] + H^+ \quad (1)$$

or as *proton transfer* from the metal ion-hydrate to some base, such as water:

$$M^{n+}[OH_2] + H_2O \rightarrow M^{n+}[OH^-] + H_3O^+ \quad (2)$$

In either case, the stronger the bonding in the hydroxide relative to that in the hydrate, the more the deprotonation of the hydrate is favored. For a full understanding of the mechanism of action of these metalloenzymes and other processes that depend on deprotonation, detailed knowledge of the fundamental nature of metal ion-hydrate and metal ion-hydroxide ion bonding is required.

The metal ion−water interaction has been studied extensively by many investigators.[5−40] Computational studies have concentrated on hydrates involving several inner sphere water molecules, e.g., $Be[OH_2]_4^{2+}$, $Mg[H_2O]_6^{2+}$, $Ca[OH_2]_6^{2+}$, $Mn[OH_2]_6^{2+}$, and $Zn[OH_2]_6^{2+}$;[25,41−46] on monohydrates in a specific group or period;[19,20,23,24,26,27] on the boundary between the first and second hydration shells;[28,34,46] on the energies of sequential hydration;[47] on proton transfer between the water molecules in the dihydrates, $M[OH_2]_2^{2+}$, where M is Be, Mg, Ca, Sr, and Ba;[48] and on the structure of the second hydration sphere, e.g., $Mg[OH_2]_6^{2+}[OH_2]_{12}$.[49−51] However, there have been far fewer computational studies of metal ion-hydroxide bonding.[26,46,52] Magnusson and Moriarty[26] have studied the mono- and divalent first-row transition metal hydroxides at the MP2/6-311+G** level with no core electron correlation and report some interesting variations, e.g. the triatomic structures of $M^{2+}[OH^-]$ are found to be linear for M = Sc, Ti, Mn, and Fe, but bent for M = V, Cr, Co, Ni, Cu, and Zn. Ricca and Bauschlicher[53] have used density functional theory and the B3LYP procedure to calculate successive OH binding energies at the CCSD(T) level for the hydroxide species $M(OH)_n^+$ with $n = 1$, 2, and 3, and M = Sc, Ti, V, Co, Ni, and Cu.

To extend these studies, and in particular to determine the effect of progressive occupancy of the s-, p-, and d-orbitals along with the creation of filled valence shells, we have carried out comprehensive calculations at the same computational level for the hydrates and hydroxides of the mono- and divalent metal ions in groups 1A, 2A, 3A, and 4A in the second, third, and fourth periods, and in the first transition series. In our earlier publication (part 1[27]) we reported structural parameters, vibrational frequencies, bonding enthalpies, orbital occupancies and energies, atomic charge distributions, and electronic charge transfers for monohydrates of metal ions. In this paper, part 2, we report corresponding data for the deprotonated species, that is, the metal ion monohydroxides, and utilize the results for both the hydrates and the hydroxides to evaluate enthalpies of deprotonation (proton dissociation and proton transfer).

Computational Methods

Ab initio molecular orbital calculations on the hydroxides, $M^{n+}[OH^-]$ with $n = 1$ and 2, were performed at the MP2(FULL)/6-311++G**//

(5) Kebarle, P. *Modern Aspects of Electrochemistry*; Conway, B. E., Bockris, J. O'M., Eds.; Plenum Press: New York, 1974; Vol. 9, p 1.
(6) Marcus, Y. *Ion Solvation*; Wiley-Interscience: Chichester, U.K., 1985; Chapter 2, p 13.
(7) Searles, S. K.; Kebarle, P. *J. Phys. Chem.* **1968**, *72*, 742−743.
(8) Dzidic, I.; Kebarle, P. *J. Phys. Chem.* **1970**, *74*, 1466−1474.
(9) Kebarle, P. *Annu. Rev. Phys. Chem.* **1977**, *28*, 455−476.
(10) Holland, P. M.; Castleman, A. W., Jr. *J. Am. Chem. Soc.* **1980**, *102*, 6174−6175.
(11) Holland, P. M.; Castleman, A. W., Jr. *J. Chem. Phys.* **1982**, *76*, 4195−4205.
(12) Burnier, R. C.; Carlin, T. J.; Reents, W. D., Jr.; Cody, R. B.; Lengel, R. K.; Freiser, B. S. *J. Am. Chem. Soc.* **1979**, *101*, 7127−7129.
(13) Magnera, T. F.; David, D. E.; Stulik, D.; Orth, R. G.; Jonkman, H. T.; Michl, J. *J. Am. Chem. Soc.* **1989**, *111*, 5036−5043.
(14) Magnera, T. F.; David, D. E.; Michl, J. *J. Am. Chem. Soc.* **1989**, *111*, 4100−4101.
(15) Marinelli, P. J.; Squires, R. R. *J. Am. Chem. Soc.* **1989**, *111*, 4101−4103.
(16) Dalleska, N. F.; Honma, K.; Sunderlin, L. S.; Armentrout, P. B. *J. Am. Chem. Soc.* **1994**, *116*, 3519−3528.
(17) Steel, E. A.; Merz, K. M., Jr.; Selinger, A.; Castleman, A. W., Jr. *J. Phys. Chem.* **1995**, *99*, 7829−7836.
(18) Hermansson, K.; Olovsson, I. *Theor. Chim. Acta (Berlin)* **1984**, *64*, 265−276.
(19) Rossi, M.; Bauschlicher, C. W., Jr. *J. Chem. Phys.* **1989**, *90*, 7264−7272.
(20) Rossi, M.; Bauschlicher, C. W., Jr. *J. Chem. Phys.* **1990**, *92*, 1876−1878.
(21) Bauschlicher, C. W., Jr.; Langhoff, S. R.; Partridge, H. In *Modern Electronic Structure Theory Part I*; Yarkony, D. R., Ed. World Scientific: Singapore, 1997; pp 1312−1318.
(22) Ricca, A.; Bauschlicher, C. W., Jr. *J. Phys. Chem.* **1995**, *99*, 9003−9007.
(23) Glendening, E. D.; Feller, D. *J. Phys. Chem.* **1995**, *99*, 3060−3067.
(24) Feller, D.; Glendening, E. D.; Kendall, R. A.; Peterson, K. A. *J. Chem. Phys.* **1994**, *100*, 4981−4997.
(25) Pavlov, M.; Siegbahn, P. E. M.; Sandström, M. *J. Phys. Chem. A* **1998**, *102*, 219−228.
(26) Magnusson, E.; Moriarty, N. W. *Inorg. Chem.* **1996**, *35*, 5711−5719.
(27) Trachtman, M.; Markham, G. D.; Glusker, J. P.; George, P.; Bock, C. W. *Inorg. Chem.* **1998**, *37*, 4421−4431.
(28) Hartman, M.; Clark, T.; van Eldik, R. *J. Am. Chem. Soc.* **1997**, *119*, 7843−7850.
(29) Marcos, E. S.; Pappalardo, R. R.; Rinaldi, D. *J. Phys. Chem.* **1991**, *95*, 8928−8932.
(30) Furuki, T.; Sakurai, M.; Inoue, Y. *J. Comput. Chem.* **1995**, *16*, 378−384.
(31) Pappalardo, R. R.; Marcos, E. S. *J. Phys. Chem.* **1993**, *97*, 4500−4504.
(32) Marini, G. W.; Texler, N. R.; Rode, B. M. *J. Phys. Chem.* **1996**, *100*, 6808−6813.
(33) Magnusson, E. *J. Phys. Chem.* **1994**, *98*, 12558−12569.
(34) Markham, G. D.; Glusker, J. P.; Bock, C. L.; Trachtman, M.; Bock, C. W. *J. Phys. Chem.* **1996**, *100*, 3488−3497.
(35) Rodriguez-Cruz, S. E.; Jockusch, R. A.; Williams, E. R. *J. Am. Chem. Soc.* **1999**, *121*, 1986−1987.
(36) Peschke, M.; Blades, A. T.; Kebarle, P. *J. Phys. Chem. A* **1998**, *102*, 9978−9985.
(37) Peschke, M.; Blades, A. T.; Kebarle, P. *J. Am. Chem. Soc.* **2000**, *122*, 10440−10449.
(38) Rotzinger, F. P. *J. Am. Chem. Soc.* **1997**, *119*, 5230−5238.
(39) Munoz-Paez, A.; Pappalardo, R. R.; Marcos, E. S. *J. Am. Chem. Soc.* **1995**, *117*, 11710−11720.
(40) Tongraar, A.; Liedl, K. R.; Rode, B. M. *J. Phys. Chem. A* **1998**, *102*, 10340−10347.
(41) Hashimoto, K.; Yoda, N.; Iwata, S. *J. Chem. Phys.* **1987**, *116*, 193−202.
(42) Bock, C. W.; Glusker, J. P. *Inorg. Chem.* **1993**, *32*, 1242−1250.
(43) Bock, C. W.; Kaufman, A.; Glusker, J. P. *Inorg. Chem.* **1994**, *33*, 419−427.
(44) Bock, C. W.; Katz, A. K.; Glusker, J. P. *J. Am. Chem. Soc.* **1995**, *117*, 3754−3765.
(45) Katz, A. K.; Glusker, J. P.; Beebe, S. A.; Bock, C. W. *J. Am. Chem. Soc.* **1996**, *118*, 5752−5763.
(46) Bock, C. W.; Katz, A. K.; Markham, G. D.; Glusker, J. P. *J. Am. Chem. Soc.* **1999**, *121*, 7360−7372.
(47) Tachikawa, H.; Ichikawa, T.; Yoshida, H. *J. Am. Chem. Soc.* **1990**, *112*, 982−987.
(48) Beyer, M.; Williams, E. R.; Bondybey, V. E. *J. Am. Chem. Soc.* **1999**, *121*, 1565−1573.
(49) Rudolph, W. W.; Pye, C. C. *J. Phys. Chem. B* **1998**, *102*, 3564−3573.
(50) Pye, C. C. *Int. J. Quantum Chem.* **2000**, *76*, 62−76.
(51) Rudolph, W. W.; Pye, C. C. *Phys. Chem. Chem. Phys.* **1999**, *1*, 4583−4593.
(52) Katz, A.; Glusker, J. P.; Markham, G. D.; Bock, C. W. *J. Phys. Chem. B* **1998**, *102*, 6342−6350.
(53) Ricca, A.; Bauschlicher, C. W. *J. Phys. Chem. A* **1997**, *101*, 8949−8955.

MP2(FULL)/6-311++G** level[54,55a−e] on CRAY computers at the National Cancer Institute and DEC alpha 3000/600 and SGI origin 2000 workstations using the GAUSSIAN 94 and 98 programs.[56] The corresponding results for the monohydrates, $M^{n+}[OH_2]$ can be found in the Supporting Information of our previous publication.[27] As noted by Kaupp and von Schleyer,[57] d-orbitals and core polarization are both important in cationic d^0 metal complexes such as $Ca^{2+}[OH_2]$. Spin projected energies (PMP2-0) were used where appropriate in these calculations on hydroxides,[56] and spin conservation was assumed in all the deprotonation reactions. Complete optimizations were performed on all the hydroxides, and frequency analyses were carried out to check whether the reported structures are local minima on the MP2(FULL)/6-311++G** potential energy surface and to evaluate the thermal energy contributions necessary for the calculations of enthalpy changes for the deprotonation processes at 298 K. Since calculations at the MP2(FULL)/6-311++G** level do not always predict the correct electronic configuration for the ground state of some first-row transition metals,[21,26,27] single point CCSD(T)(FULL)/6-311++G**//MP2(FULL)/6-311++G** calculations were performed in order to treat the effects of electron correlation in evaluating deprotonation enthalpies more completely. For brevity in the main text, the calculations at these two levels will be referred to as "MP2" and "CCSD(T)", respectively. Optimizations were also carried out using density functional theory (DFT) at the B3LYP/6-311++G** computational level for certain examples. This DFT approach, however, can have different biases with respect to the relative occupation of the 4*s* and 3d orbitals from those found by the use of second-order Møller−Plesset perturbation theory.[25,58] Natural population analyses (NPA) were employed to calculate atomic charges from the MP2(FULL)/6-311++G** electron density;[59−61] natural bond orbitals (NBOs), constructed from the HF/6-311++G** density, were used to examine metal ion-oxygen bonding. Coordinate systems for the two types of hydroxide structure, bent and linear, are depicted in Figure 1.

The most demanding calculations were those for the transition metal hydroxides as a consequence of the various possible occupations of the 3d- and 4s-orbitals which increase the number of competing bonding mechanisms. As pointed out by Bauschlicher and Langhoff,[62,63] accurate descriptions of molecules containing transition metal atoms or ions generally require sophisticated computational methods, particularly when there is a large covalent contribution to the bonding. For example, the modified coupled-pair functional (MCPF), coupled cluster (CC), and multireference configuration interaction (MRCI) approaches usually provide reliable results for such molecules.[64−66] We have used the CCSD(T)(FULL)/6-311++G** computational level that includes a perturbational estimate of connected triple excitations, at the MP2(FULL)/6-311++G** optimized geometry. This computational level gives reasonable binding energies in transition metal systems.[27,63,64] For most of the transition metal ions several multiplicities and electronic configurations were considered, although it was not practicable to study all possible electronic states for each hydroxide.

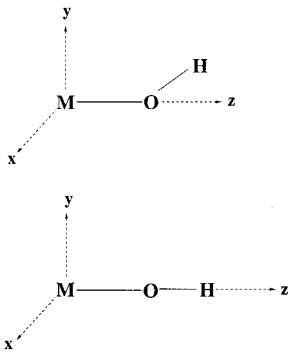

Figure 1. Coordinate systems for bent and linear $M^{n+}[OH^-]$.

For the proton transfer (deprotonation) process, $M^{n+}[OH_2] + H_2O \rightarrow M^{n+}[OH^-] + H_3O^+$, we report enthalpy changes at 298 K for the metal ion hydrates with the lowest CCSD(T)(FULL)/6-311++G**//MP2(FULL)/6-311++G** energy.[27] *Spin conservation* was enforced in all of these calculations. In a few instances, we found that the lowest energy form of a metal ion hydroxide had a different spin multiplicity from that found for the corresponding metal ion hydrate. When this occurs, it is noted in the tables.

Results

Some of the results of our studies are listed in Supporting Information as follows: The total molecular energies, thermal corrections, and entropies at the MP2 level for the main group metal ion hydroxides, $M^{n+}[OH^-]$, $n = 1$ or 2, are given in Table 1SA; total molecular energies at the CCSD(T) level are also given in this table. Analogous data for a variety of electronic states for the transition metal ion hydroxides are given in Table 1SB, along with the NPA populations of the 3d and 4s orbitals. Total molecular energies and orbital occupancies for several of the transition metal hydroxides using density functional theory (DFT) at the B3LYP/6-311++G** level are listed in Table 2S. The data analogous to those in Table 1S for the corresponding metal ion monohydrates, and for the mono- and divalent metal ions, have already been published by us.[27]

A. Geometrical Parameters. Geometries (M−O and O−H distances and MOH angles) and binding enthalpies (ΔH°_{298}) found for the metal ion hydroxides ($M^{n+}[OH^-]$ with $n = 1$ and 2) in main groups 1A, 2A, 3A, and 4A of the first, second, and third periods are listed in Table 1A. Corresponding values for the transition metal ion hydroxides of the fourth period are given in Table 1B with the data for calcium and zinc included for

(54) Møller, C.; Plesset, M. S. *Phys. Rev.* **1934**, *46*, 618−622.
(55) (a) McLean, A. D.; Chandler, G. S. *J. Chem. Phys.* **1980**, *72*, 5639−5648. (b) Krishnan, R.; Binkley, J. S.; Seeger, R.; Pople, J. A. *J. Chem. Phys.* **1980**, *72*, 650−654. (c) Wachters, A. J. H. *J. Chem. Phys.* **1970**, *52*, 1033−1036. (d) Hay, P. J. *J. Chem. Phys.* **1977**, *66*, 4377−4384. (e) Raghavachari, K.; Trucks, G. W. *J. Chem. Phys.* **1989**, *91*, 1062−1065.
(56) Frisch, M. J.; Trucks, G. W.; Schlegel, H. B.; Gill, P. M. W.; Johnson, B. G.; Robb, M. A.; Cheeseman, J. R.; Keith, T. A.; Peterson, G. A.; Montgomery, J. A.; Raghavachari, K.; Al-Laham, M. A.; Zakrzewski, V. G.; Ortiz, J. V.; Foresman, J. B.; Cioslowski, J.; Stefanov, B. B.; Nanayakkara, A.; Challacombe, M.; Peng, C. Y.; Ayala, P. Y.; Chen, W.; Wong, M. W.; Andres, J. L.; Replogle, E. S.; Gomperts, R.; Martin, R. L.; Fox, D. J.; Binkley, J. S.; Defrees, D. J.; Baker, J.; Stewart, J. P.; Head-Gordon, M.; Gonzales, C.; Pople, J. A. *GAUSSIAN 94*, Revision A.1; Gaussian, Inc.: Pittsburgh, PA, 1995. Frisch, M. J.; Trucks, G. W.; Schlegel, H. B.; Scuseria, G. E.; Robb, M. A.; Cheeseman, J. R.; Zakrzewski, V. G.; Montgomery, J. A.; Stratmann, R. E.; Burant, J. C.; Dapprich, S.; Millam, J. M.; Daniels, A. D.; Kudin, K. N.; Strain, M. C.; Farkas, O.; Tomasi, J.; Barone, V.; Cossi, M.; Cammi, R.; Mennucci, B.; Pomelli, C.; Adamo, C.; Clifford, S.; Ochterski, J.; Peterson, G. A.; Ayala, P. Y.; Cui, Q.; Morokuma, K.; Malick, D. K.; Rabuck, A. D.; Raghavachari, K.; Foresman, J. B.; Cioslowski, J.; Ortiz, J. V.; Stefanov, B. B.; Liu, G.; Liashenko, A.; Piskorz, P.; Komaromi, I.; Gomperts, R.; Martin, R. L.; Fox, D. J.; Keith, T.; Al-Laham, M. A.; Peng, C. Y.; Nanayakkara, A.; Gonzalez, C.; Challacombe, M.; Gill, P. M. W.; Johnson, B. G.; Chen, W.; Wong, M. W.; Andres, J. L.; Head-Gordon, M.; Replogle, E. S. and Pople, J. A. *Gaussian 98*, Revision A.1; Gaussian Inc.: Pittsburgh, PA, 1998.
(57) Kaupp, M.; Schleyer, P. v. R. *J. Chem. Phys.* **1992**, *96*, 7316−7323.
(58) Ricca, A.; Bauschlicher, C. W., Jr. *J. Phys. Chem.* **1994,** *98*, 12899−12903.
(59) Reed, A. E.; Curtiss, L. A.; Weinhold, F. *Chem. Rev.* **1988**, *88*, 899−926.
(60) Reed, A. E.; Weinstock, R. B.; Weinhold, F. *J. Chem. Phys.* **1985**, *83*, 735−746.
(61) Glendening, E. D.; Reed, A. E.; Carpenter, J. E.; Weinhold, F. *NBO*, Version 3.1.
(62) Bauschlicher, C. W., Jr.; Langhoff, S. R. *Int. Rev. Phys. Chem.* **1990**, *9*, 149−185.
(63) Langhoff, S. R.; Bauschlicher, C. W., Jr. *Annu. Rev. Phys. Chem.* **1988**, *39*, 181−212.
(64) Chong, D. P.; Langhoff, S. R. *J. Chem. Phys.* **1986**, *84*, 5606−5610.
(65) Bartlett, J. *Annu. Rev. Phys. Chem.* **1981**, *32*, 359−410.
(66) *Lecture Notes in Quantum Chemistry*; Roos, B. O., Ed.; Springer: Heidelberg, 1992.

Table 1. Bond Lengths (Å), Bond Angles (deg), and Bonding Enthalpies, ΔH°_{298} (kcal/mol). Metal Ion Monohydroxides Calculated at the MP2(FULL)/6-311++G**//MP2(FULL)/6-311++G** and {CCSD(T)(FULL)/6-311++G**//MP2(FULL)/6-311++G**} Computational Levels

A. Main Group

period	*n*		group 1A	group 2A	group 3A	group 4A	*n*		group 2A	group 3A	group 4A
2	1	M	Li^{n+}	Be^{n+}	B^{n+}	C^{n+}	2	M	Be^{n+}	B^{n+}	C^{n+}
		state	$^1\Sigma^+$	$^2A'$	$^1A'$	$^2A'$		state	$^1\Sigma^+$	$^2\Sigma^+$	$^1\Sigma^+$
		M−O	1.602	1.416	1.307	1.279		M−O	1.330	1.220	1.162
		O−H	0.952	0.953	0.966	0.977		O−H	0.958	0.972	0.996
		∠MOH	180.0	135.1	116.8	111.5		∠MOH	180.0	180.0	180.0
		ΔH°_{298}	−187.0	−275.0	−305.1	−343.5		ΔH°_{298}	−505.5	−653.3	−723.1
			{−187.8}	{−278.1}	{−306.0}	{−340.4}			{−507.6}	{−658.3}	{−716.9}
3	1	M	Na^{n+}	Mg^{n+}	Al^{n+}	Si^{n+}	2	M	Mg^{n+}	Al^{n+}	Si^{n+}
		state	$^1\Sigma^+$	$^2\Sigma^+$	$^1A'$	$^2A'$		state	$^1\Sigma^+$	$^2\Sigma^+$	$^1\Sigma^+$
		M−O	1.972	1.805[a]	1.705[b]	1.670		M−O	1.731[c]	1.619	1.552
		O−H	0.954	0.950[a]	0.953[b]	0.962		O−H	0.952[c]	0.958	0.968
		∠MOH	180.0	180.0[a]	165.7[b]	119.4		∠MOH	180.0[c]	180.0	180.0
		ΔH°_{298}	−154.2	−203.3	−220.8	−252.6		ΔH°_{298}	−374.5	−443.9	−474.5
			{−154.6}	{−205.1}	{−222.4}	{−253.6}			{−375.6}	{−444.5}	{−496.4}
4	1	M	K^{n+}	Ca^{n+}	Ga^{n+}	Ge^{n+}	2	M	Ca^{n+}	Ga^{n+}	Ge^{n+}
		state	$^1\Sigma^+$	$^2\Sigma^+$	$^1A'$	$^2A'$		state	$^1\Sigma^+$	$^2A'$	$^1\Sigma^+$
		M−O	2.243	2.033	1.820[d]	1.805		M−O	1.944	1.733[e]	1.675
		O−H	0.957	0.954	0.960[d]	0.964		O−H	0.957	0.971[e]	0.968
		∠MOH	180.0	180.0	129.0[d]	113.8		∠MOH	180.0	121.8[e]	180.0
		ΔH°_{298}	−139.2	−187.8	−205.1	−236.5		ΔH°_{298}	−330.5	−442.8	−439.0
			{−139.4}	{−188.6}	{−205.4}	{−235.9}			{−330.6}	{−445.5}	{−430.0}

B. First Transition Series

period	*n*		group 2A	group 3B	group 4B	group 5B	group 6B	group 7B	group 8	group 8	group 8	group 1B	group 2B
	1	M	Ca^{n+}	Sc^{n+}	Ti^{n+}	V^{n+}	Cr^{n+}	Mn^{n+}	Fe^{n+}	Co^{n+}	Ni^{n+}	Cu^{n+}	Zn^{n+}
		state	$^2\Sigma^+$	$^3\Delta$	$^4A''$	$^5A''$ [r]	$^6A'$ [o]	$^7A'$	$^6A'$	$^3A'$	$^2A'$	$^1A'$	$^2A'$
		M−O	2.033	1.885[f]	1.852	1.810	1.804	1.853	1.811	1.786	1.779	1.768	1.817
		O−H	0.954	0.954[f]	0.957	0.960	0.960	0.954	0.956	0.961	0.961	0.962	0.962
		∠MOH	180.0	180.0[f]	145.9	133.1	122.0	155.9	140.0	119.9	116.0	111.1	114.9
		ΔH°_{298}	−187.8	−211.6	−211.2	−213.3	−181.4	−203.0	−213.4	−175.7	−159.0	−204.8	−212.6
			{−188.6}[i]	{−213.6}[i]	{−214.9}[i]	{−219.5}[i] {−213.3}[j]	{−205.2}[j] {−240.7}[i]	{−201.3}[g,i]	{−217.2}[h,i]	{−206.2}[j] {−233.6}[i]	{−206.2}[j] {−242.0}[i] {−204.7}[p]	{−200.8}[k] {−229.6}[l]	{−214.3}[i]
4	2	state	$^1\Sigma^+$	$^2\Sigma^+$	$^3\Delta$	$^4\Sigma^-$	$^5A'$	$^6A'$	$^5A'$	$^4A'$	$^3A''$	$^2A''$	$^1A'$
		M−O	1.944	1.746	1.714	1.710	1.745	1.764	1.713	1.718[m]	1.719	1.675[n]	1.759
		O−H	0.957	0.967	0.967	0.966	0.964	0.961	0.962	0.967[m]	0.966	0.972[n]	0.972
		∠MOH	180.0	180.0	180.0	180.0	134.3	141.7	141.5	124.1[m]	123.3	122.9[n]	112.7
		ΔH°_{298}	−330.5	−370.6	−374.9	−379.5	−397.1	−383.0	−403.9	−416.4	−413.8	−433.2	−421.1
			{−330.6}[q]	{−371.0}	{−379.3}	{−385.7}	{−401.5}	{−387.0}	{−406.1}	{−421.7}	{−432.9}	{−446.1}[n]	{−421.4}

[a] At the B3LYP/6-311++G**//B3LYP/6-311++G** level: Mg−O = 1.799 Å; O−H = 0.951 Å; ∠MgOH = 180°. [b] At the B3LYP/6-311++G**//B3LYP/6-311++G** level: Al−O = 1.706 Å; O−H = 0.953 Å; ∠AlOH = 166.3°. [c] At the B3LYP/6-311++G**//B3LYP/6-311++G** level: Mg−O = 1.727 Å; O−H = 0.956 Å; ∠MgOH = 174.3°. [d] At the B3LYP/6-311++G**//B3LYP/6-311++G** level: Ga−O = 1.832 Å; O−H = 0.960 Å; ∠GaOH = 135.7°. [e] At the B3LYP/6-311++G**//B3LYP/6-311++G** level: Ga−O = 1.817 Å; O−H = 0.977 Å; ∠GaOH = 118.0°. [f] At all levels of computation the singlet state for $Sc^+[OH^-]$ was found to have the lowest energy; see Table 1S of the Supporting Information. The geometrical parameters for this state are as follows: M−O, 1.819 Å; O−H, 0.971 Å; ∠MOH = 180.0°. [g] At the CCSD(T) level, the lowest energy of $Mn^+[OH_2]$ is for the $^7A_1$ state. If the $^5A_1$ state is used, ΔH°_{298} for the deprotonation is 213.5 {217.6} kcal/mol. [h] At the CCSD(T) level, the lowest energy of $Fe^+[OH_2]$ is for the $^6A_1$ state. If the $^4B_2$ state is used, ΔH°_{298} for the deprotonation is +231.1{+216.4} kcal/mol and if the $^4A_1$ state is used ΔH°_{298} is 207.9{218.3} kcal/mol. [i] Calculated using the lowest energy ($4s^13d^n$) state of the metal hydroxide, $M^+[OH^-]$ and the corresponding ($4s^13d^n$) state of the isolated metal ion, M^+. [j] Calculated using the lowest energy ($4s^13d^n$) states of the metal hydroxide, $M^+[OH^-]$, and the lowest energy state ($4s^03d^{n+1}$) of the isolated metal ion M^+. [k] Calculated using the lowest energy ($4s^03d^{10}$) state of $Cu^+[OH^-]$ and the corresponding ($4s^03d^{10}$) state of the isolated Cu^+ ion. [l] Calculated value using the triplet states of Cu^+ and $Cu^+[OH^-]$ with $4s3d_{Z^2}$ occupancy. [m] At the MP2 computational level, quintic states are lower in energy than the triplet state; see Table 2S of the Supporting Information. The structural parameters for the lowest quintic state are: Co^+−O = 1.813 Å; O−H = 0.959 Å; ∠CoOH = 125.1°. [n] The geometry for $Cu^{2+}[OH^-]$ using the lowest energy value at the MP2 level (see Table 2S) are as follows: Cu^{2+}−O = 1.688 Å; O−H = 0.969 Å; ∠CuOH = 116.9°. [o] Attempts to find a $4s^03d^5$ state for $Cr^+[OH^-]$ repeatedly resulted in a state better described as $4s^13d^4$. This is contrary to what we observed for $Cr^+[OH_2]$.[27] [p] This value was obtained using the state of $Ni^+[OH^-]$ ($3d^9$) which is lowest in energy at the MP2(FULL)/6-311++G** levels (see Table 1SB) and the corresponding state of the Ni^+ ion. This is the state used by Magnusson and Moriarty.[26] [q] At the B3LYP/6-311++G**//B3LYP/6-311++G** computational level, ΔH°_{298} = −343.0 kcal/mol; at the B3LYP/6-311++G(2d,2p)//B3LYP/6-311++G(2d,2p) level, ΔH°_{298} = −346.1 kcal/mol. [r] The calculated splitting $^5D(S°) - {}^5F(S^1)$ for the isolated V^+ ion is 0.27 ev at the CCSD(T) level; the experimental value is 0.33 eV.[68]

comparison. The NPA electronic configuration of the lowest energy states are best described as $4s^13d^n$ (n = 0−10) for hydroxides of Ca to Zn in the monovalent state. These were calculated at the MP2 level; this configuration helps to maximize the spin multiplicity. The only exception is singlet $Cu^+[OH^-]$, where the electronic configuration is more like $4s^03d^{10}$ (the population of the 4s orbital is 0.34; see Table 1SB). Various triplet states of $Cu^+[OH^-]$ that have an electronic configuration which is essentially $4s^13d^9$ are found to be much higher in energy than the singlet state. For the corresponding divalent metal hydroxides the electronic configurations are all best described as $4s^03d^n$ (n = 0−10). Thus, the 4s electron of the monovalent state is lost on oxidation.

Our previous calculations (also at the MP2 level) had indicated that ground-state structures of all the M^+ and M^{2+} metal ions bound to a water molecule have all four atoms

Chart 1. Summary of Trends in Molecular Geometries of the Main Group Metal Ion Monohydroxides

	Group 1A → 2A → 3A → 4A	2nd period → 3rd → 4th
M-O distance (Å)	decrease	increase
O-H distance (Å)	increase	*
∠ MOH bond angle (°)	remains at 180° or decreases	*
Deprotonation enthalpy, ΔH°_{298} (kcal/mol)	decreases	increases

*No trend is evident in these two cases

Table 2. Atomic Charges, *q*, on M, O, and H and the Transfer of Electronic Charge from the HO to the Metal Ion. Metal Ion. Metal Ion Monohydroxides, $M[OH]^{(n-1)+}$ with $n = 1$ and 2, Calculated from Natural Population Analyses (NPA) Using the MP2(FULL)/6-311++G** Densities

A. In the Main Group

		$n = 1$				$n = 2$			
period	M	q_M	q_O	q_H	transfer	q_M	q_O	q_H	transfer
2	Li	+0.960	−1.408	+0.447	+0.039	–	–	–	–
	Be	+0.892	−1.388	+0.496	+0.108	+1.807	−1.371	+0.564	+0.194
	B	+0.464	−0.984	+0.521	+0.531	+1.267	−0.893	+0.626	+0.732
	C	+0.196	−0.674	+0.477	+0.804	+0.886	−0.555	+0.669	+1.115
3	Na	+0.984	−1.417	+0.431	+0.015	–	–	–	–
	Mg	+0.982	−1.459	+0.476	+0.018	+1.920	−1.439	+0.518	+0.080
	Al	+0.814	−1.316	+0.501	+0.186	+1.715	−1.276	+0.561	+0.185
	Si	+0.629	−1.112	+0.483	+0.370	+1.576	−1.168	+0.592	+0.423
4	K	+0.982	−1.409	+0.425	+0.018	–	–	–	–
	Ca	+0.984	−1.449	+0.464	+0.017	+1.883	−1.383	+0.499	+0.116
	Ga	+0.771	−1.247	+0.476	+0.229	+1.570	−1.096	+0.525	+0.430
	Ge	+0.616	−1.084	+0.468	+0.384	+1.577	−1.158	+0.581	+0.423

B. In the First Transition Series

	$n = 1$				$n = 2$			
M	q_M	q_O	q_H	transfer	q_M	q_O	q_H	transfer
Ca	+0.984	−1.449	+0.465	+0.016	+1.883	−1.383	+0.500	+0.117
Sc	+0.818	−1.298	+0.480	+0.182	+1.531	−1.070	+0.539	+0.469
Ti	+0.773	−1.246	+0.473	+0.227	+1.501	−1.034	+0.533	+0.499
V	+0.715	−1.180	+0.465	+0.285	+1.515	−1.043	+0.528	+0.485
Cr	+0.693	−1.150	+0.457	+0.302	+1.586	−1.089	+0.503	+0.414
Mn	+0.897	−1.376	+0.479	+0.103	+1.709	−1.226	+0.517	+0.291
Fe	+0.852	−1.329	+0.477	+0.148	+1.649	−1.173	+0.524	+0.351
Co	+0.777	−1.232	+0.455	+0.223	+1.613	−1.112	+0.499	+0.387
Ni	+0.809	−1.248	+0.439	+0.191	+1.634	−1.128	+0.494	+0.366
Cu	+0.778	−1.218	+0.440	+0.222	+1.537	−1.030	+0.493	+0.463
Zn	+0.828	−1.280	+0.452	+0.172	+1.612	−1.104	+0.492	+0.388

coplanar, indicative of a strong ion−dipole interaction.[27] For the corresponding hydroxides the ground-state structures of the M^+ metal hydroxides are linear for metals on the extreme left side of the Periodic Table, but are bent to an increasing extent as one proceeds toward the right of the Table; the M^{2+} metal hydroxides show a similar pattern, but linear structures generally extend further to the right in a given period; see Table 1A,B. These trends are more internally consistent than those described earlier from lower level computational results.[26] The M^{2+}−O−H angle is generally greater than or equal to the corresponding M^+−O−H angle for a given metal M, and the M−O−H angle tends to decrease from left to right in a given period.

(a) Main Group Metals. For the main group hydroxides, as the s and p valence shells are progressively filled in going from group 1A → 2A → 3A → 4A the M−O distance decreases, the O−H bond length generally increases and the MOH angle remains at 180° or decreases; see Chart 1. In these main group hydroxides the M−O bond length increases in going from the second period → third → fourth, but to a smaller extent than that observed for the corresponding hydrates (see Figure 1S);[27] no trend was apparent for either the O−H bond length or the MOH angle of the hydroxides.

An examination of the NBOs of the mono and divalent group 4A hydroxides in periods 2−4 does not indicate the presence of a formal metal−oxygen bonding orbital. For group 3A, metal−oxygen bonding orbitals are present for both the mono- and divalent boron and gallium hydroxides, but not for the aluminum hydroxide. No formal metal−oxygen bonds were found for any of the group 1A or group 2A hydroxides. The presence of a formal metal−oxygen bond correlates well with a greater transfer of charge from the hydroxide to the metal ion; see Table 2A.

(b) First-Row Transition Metals. The M−O bond distances in the first-row transition metal ion hydroxides $M^{n+}[OH^-]$ (*n*

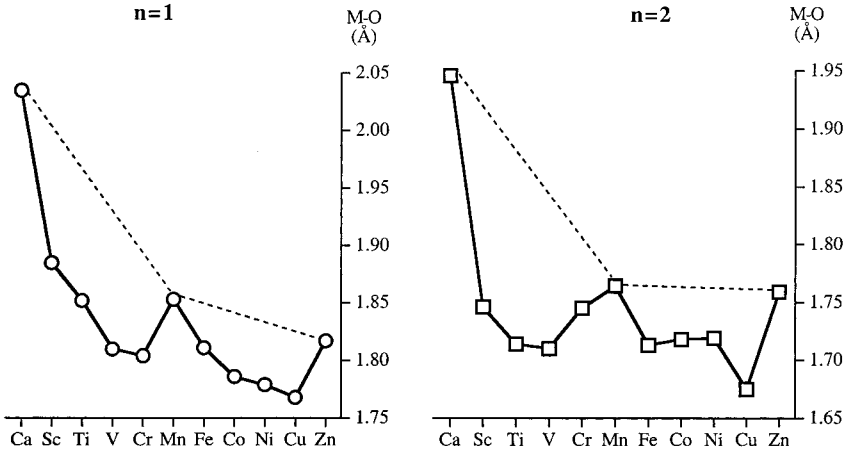

Figure 2. Variation of the M−O bond distance for the monovalent ($n = 1$) and divalent ($n = 2$) transition metal ion hydroxides calculated at the MP2(FULL)/6-311++G**//MP2(FULL)/6-311++G** level.

= 1, 2) are significantly affected as the 3d shell becomes filled. This is shown in Figure 2, where it is evident that, taking the values for Ca, Mn and Zn as reference points, these distances follow an inverted double humped curve similar to that observed for the corresponding monohydrates.[27] This double hump characteristic is a consequence of the occupation of the 3d orbitals which project well out to the periphery of the metal ions and are thus able to influence their environment significantly; hence, many of the properties of these hydroxides with partly filled d shells are sensitive to the number and arrangement of the d electrons present.

The NBOs based on the HF/6-311++G** density do not indicate the presence of a formal bond between the metal cation and the oxygen atom of the hydroxyl anion except for $Cu^+[OH^-]$, $Cr^{2+}[OH^-]$, and $Zn^{2+}[OH^-]$. Even in these three cases, however, the contribution of the metal ion to this bond is quite small (5.1, 12.0, and 10.7%, respectively). The changes in M−O bond distances across the first-row transition metals are much less pronounced for the shorter metal−oxygen distances found in the hydroxides than for the metal−oxygen distances in the corresponding hydrates (see Figure 2S).[27] These shorter M−O distances are the result of a greater electrostatic interaction in the hydroxides than in the hydrates.

NBO analyses of the metal d-orbitals in the monovalent transition metal hydroxides show a strong sd hybridization. As noted by Bauschlicher et al.[21] the $4s-3d_{z^2}$ orbital mixing reduces the charge density along the *z* axis, thereby reducing the transition metal−OH repulsion without significantly changing the *s* or d population. As noted previously, the only exception is the singlet state of cuprous hydroxide for which the electronic configuration of the copper is best described as having a filled d shell. Since the 3d orbitals are more compact than the 4s orbital, $Cu^+[OH^-]$ has the shortest M−O distance in the first-row transition metal series at the MP2 level. Interestingly, the formation of the Cu^+-O bond has the lowest exothermicity in this series as a result of the low 4s occupancy; see Table 1B and Table 1SB.

B. Vibrational Frequencies. The vibrational modes for both the linear and bent monohydroxides are depicted in Chart 2. Vibrational frequencies for the main group metal ion monohydroxides, $M^+[OH^-]$ and $M^{2+}[OH^-]$, calculated at the MP2 level are listed in Supplementary Information Table 3SA, and values for the transition metal ion monohydroxides in Table 3SB.

The M−O stretching frequencies for the first-row transition metal mono- and divalent hydroxides, $M^{n+}[OH^-]$ ($n = 1,2$), follow typical "double-humped" curves with respect to baseline

Chart 2. Vibrational Modes

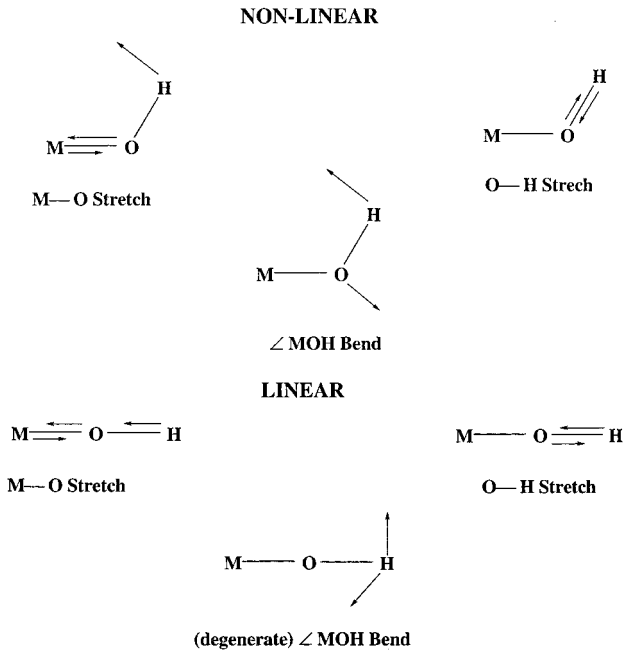

values for Ca, Mn, and Zn (see Figure 3S of the Supporting Information). However, there does not appear to be a simple linear relationship between the stretching frequencies and the inverse of the M−O distances—although such a relationship was observed in the corresponding hydrates.[27] The stronger electrostatic interactions in the hydroxides as compared to the hydrates, reflected in the significant decrease in the M−O distances by 0.15−0.20 Å, evidently permit relatively little change in this distance and the vibrational frequency associated with it throughout the series Ca to Zn.

A few of the calculated frequencies call for comment. The frequency of the Cu^+-O vibration, 617 cm^{-1}, is much lower than that for the other monovalent metal ions and can be attributed to the particular orbital occupancy. As mentioned above, NPA analysis of the lowest energy state for $Cu^+[OH^-]$ at the MP2 level shows essentially a $3d^{10}$ orbital configuration for the copper with a very low 4s occupancy. To gain some insight as to the influence that the lack of a 4s electron has on the M−O frequency, we carried out frequency analyses on both the $4s3d^8$ and $3d^9$ electronic states of $Ni^+[OH^-]$. For the $4s3d^8$ state, which has the lowest energy at the MP2 level, the M−O frequency was found to be 653 cm^{-1}; whereas with the $3d^9$

Table 3. Values of the Ratio $(q_{M(hydrate)} - q_{M(hydroxide)})/q_{M(hydrate)}$ for the Main Group and First-Row Transition Metals

	main group metals			first-row transition metals	
	$n = 1$	$n = 2$		$n = 1$	$n = 2$
Li	0.030	−	Ca	0.008	0.026
Be	0.075	0.055	Sc	0.142	0.209
B	0.416	0.213	Ti	0.182	0.219
C	0.649	0.331	V	0.230	0.210
			Cr	0.286	0.161
Na	0.011	−	Mn	0.085	0.116
Mg	0.081	0.029	Fe	0.122	0.138
Al	0.156	0.086	Co	0.197	0.152
Si	0.288	0.146	Ni	0.161	0.146
			Cu	0.200	0.180
K	0.090	−	Zn	0.082	0.160
Ca	0.008	0.026			
Ga	0.205	0.147			
Ge	0.317	0.154			

configuration the frequency is reduced to 613 cm^{-1}. This decrease in stretching frequency is in accord with a decrease (of 12.4 kcal/mol) found for the $Ni^+[OH^-]$ dissociation energy.

C. Charge Distribution. Atomic charges from NPA analyses using the MP2 density are given in Tables 2A,B for the main group and first-row transition metals, respectively. For both $n = 1$ and 2, more electron density is transferred to the metal cation from a hydroxide ion than from a water molecule. However, the ratio $(q_{M(hydrate)} - q_{M(hydroxide)})/q_{M(hydrate)}$, which emphasizes the difference between the charge transfer in the hydrates and hydroxides, varies widely; see Table 3. For the main group metals the ratio increases in going from 1A→2A→3A→4A, but decreases as the charge goes from +1 to +2; the largest value of this ratio, 0.65, occurs for the monovalent carbon ion, suggesting that the bonding in $C^+[OH^-]$ is significantly more covalent than in $C^+[OH_2]$. For the first-row transition metals this ratio follows essentially a double-humped curve in going from Ca to Zn.

It is interesting to compare charge transfer in the complexes $Cr^+[OH^-]$ and $Cr^+[OH_2]$ (which have a ratio of 0.29) with those in $Mn^+[OH^-]$ and $Mn^+[OH_2]$ (which have a much smaller ratio of 0.08). In $Cr^+[OH_2]$ the occupancy of the 4s orbital is low, only about 0.1, whereas the 3d orbitals are essentially half-filled with an occupancy of 4.9. For $Cr^+[OH^-]$; however, the occupancy of the 4s orbital is greater, 0.9, while that of the 3d orbital has decreased to a value of 4.4, a result of significant $4s-3d_{Z^2}$ hybridization. On the other hand, the occupancies of the 4s and 3d orbitals for $Mn^+[OH_2]$ and $Mn^+[OH^-]$ are nearly the same. It may be noted that the enthalpy of formation of $Cr^+[OH^-]$, −240.7 kcal/mol, is much more exothermic than that of $Mn^+[OH^-]$, −201.3 kcal/mol, when the orbital occupancy of the chromium in both the isolated ion and the corresponding hydroxide are nearly the same ($4s3d^4$); see Table 1B.

D. Bonding Enthalpies. The values of ΔH°_{298} for the formation of the mono- and divalent main group metal ion hydroxides are given in Table 1A and those for the transition metal ion hydroxides in Table 1B. For a particular metal ion charge, the increase in ΔH°_{298} for the main group hydroxides as the M−O bond distance decreases is well-represented by the same inverse linear relationship as that found for the hydrates, $\Delta H^\circ_{298} = A + B(1/M-O)$; see Figure 3. The values for the parameters A and B and the correlation coefficients, r, are listed in Table 4S of the Supporting Information.

To analyze trends in the formation enthalpies of the transition metal ion hydroxides in going from Ca^{n+} to Zn^{n+}, we consistently chose states in which the electron occupancy of the 4s orbital of the isolated metal ion was similar to that in the lowest-energy state of corresponding hydroxide. This choice was not an issue in the case of the divalent ions and their hydroxides because the occupancy of the 4s orbital in all of their lowest-energy states is quite small; see Table 2SB of the Supporting Information. The variation of ΔH°_{298} in going from $Ca^{2+}[OH^-]$ to $Zn^{2+}[OH^-]$, as shown in Figure 4B, follows the expected double-humped curve with respect to the values for $Ca^{2+}[OH^-]$, $Mn^{2+}[OH^-]$, and $Zn^{2+}[OH^-]$ as reference. On the other hand, the monovalent hydroxides $M^+[OH^-]$ and the corresponding ions present problems. The occupancy of the 4s orbital in the lowest energy states of all the monovalent hydroxides (except for $Cu^+[OH^-]$) is nearly unity. For the isolated monovalent ions of Ca, Sc, Ti, Mn, Fe, and Zn the 4s occupancy is also nearly unity, but for the monovalent ions of V, Cr, Co, Ni, and Cu this occupancy is very low in agreement with experiment.[67,68] As a consequence, the bonding enthalpies for $V^+[OH^-]$, $Cr^+[OH^-]$, $Co^+[OH^-]$, and $Ni^+[OH^-]$ calculated using the lowest-energy states of the corresponding monovalent ions necessarily contain a contribution from electron reorganization involving the 4s and 3d orbitals. The difference in the ΔH°_{298} value for $V^+[OH^-]$ is only about 6 kcal/mol; for $Cr^+[OH^-]$, $Co^+[OH^-]$, and $Ni^+[OH^-]$ the differences are sufficiently large that no "hump" is observed between $Mn^+[OH^-]$ and $Zn^+[OH^-]$; see Figure 4A. Further enthalpy calculations using energies for the lowest excited states of the Cr^+, Co^+, and Ni^+ ions in which the 4s orbital occupancy more closely matches that of the corresponding hydroxide increases the exothermicity of ΔH°_{298} for the formation of the Cr−O, Co−O, and Ni−O bonds by 35.5, 27.4, and 35.8 kcal/mol, respectively. The situation with Cu^+ and $Cu^+[OH^-]$ is somewhat unique since the lowest-energy states of both species have relatively low 4s occupancy. The value of ΔH°_{298} for the formation of the Cu−O bond using these states is the smallest we observed for the monovalent metal hydroxides. However, when energies for the excited triplet states of Cu^+ and $Cu^+[OH^-]$ ($4s^13d^9$) states are used we find a ΔH°_{298} value of −229.6 kcal/mol instead of −200.8 kcal/mol calculated at the CCSD(T) level. Incorporating these alternative values for Cr, Co, Ni, and Cu, the traditional double-humped curve is now evident; see Figure 4A.

CCSD(T) ligand field stabilization energies for $Fe^{2+}[OH^-]$, $Co^{2+}[OH^-]$, $Ni^{2+}[OH^-]$, and $Cu^{2+}[OH^-]$ have been evaluated using the ΔH°_{298} values for $Mn^{2+}[OH^-]$ and $Zn^{2+}[OH^-]$ as baseline. In Table 4[27,69] these values, 12, 21, 25, and 32 kcal/mol respectively are compared with the values calculated for the monohydrate, the experimental values for the aqueous hexaaquoion, and values derived from the lattice energies for the fluoride, chloride, and oxide crystals. It is quite striking that, with only one anionic ligand, OH^-, the values approach those for the multianion interactions in a crystalline environment.

The double-humped variation of ΔH°_{298} in going from $Ca^{n+}[OH^-]$ to $Zn^{n+}[OH^-]$ is accompanied by an inverted double-humped variation of the M−O bond length, as can be seen by comparing Figures 2 and 4. Plots of ΔH°_{298} versus 1/M−O are given in Figure 5. Excluding $Ca^+[OH^-]$ and $Sc^+[OH^-]$, which are linear structures, the values of ΔH°_{298} for the bent structures, $Ti^+[OH^-]$ through $Zn^+[OH^-]$, show a good linear dependence on 1/M−O in accord with eq 1; the

(67) Moore, C. E. *Atomic Energy Levels*; U.S. Department of Commerce, National Bureau of Standards, U. S. GPO: Washington, D.C., 1952, 1958.
(68) Blomberg, M. R. A.; Siegbahn, Per E. M.; Svensson, M. *J. Chem. Phys.* **1996**, *104*, 9546−9554.
(69) George, P.; McClure, D. S. *Prog. Inorg. Chem.* **1959**, *1*, 381−463.

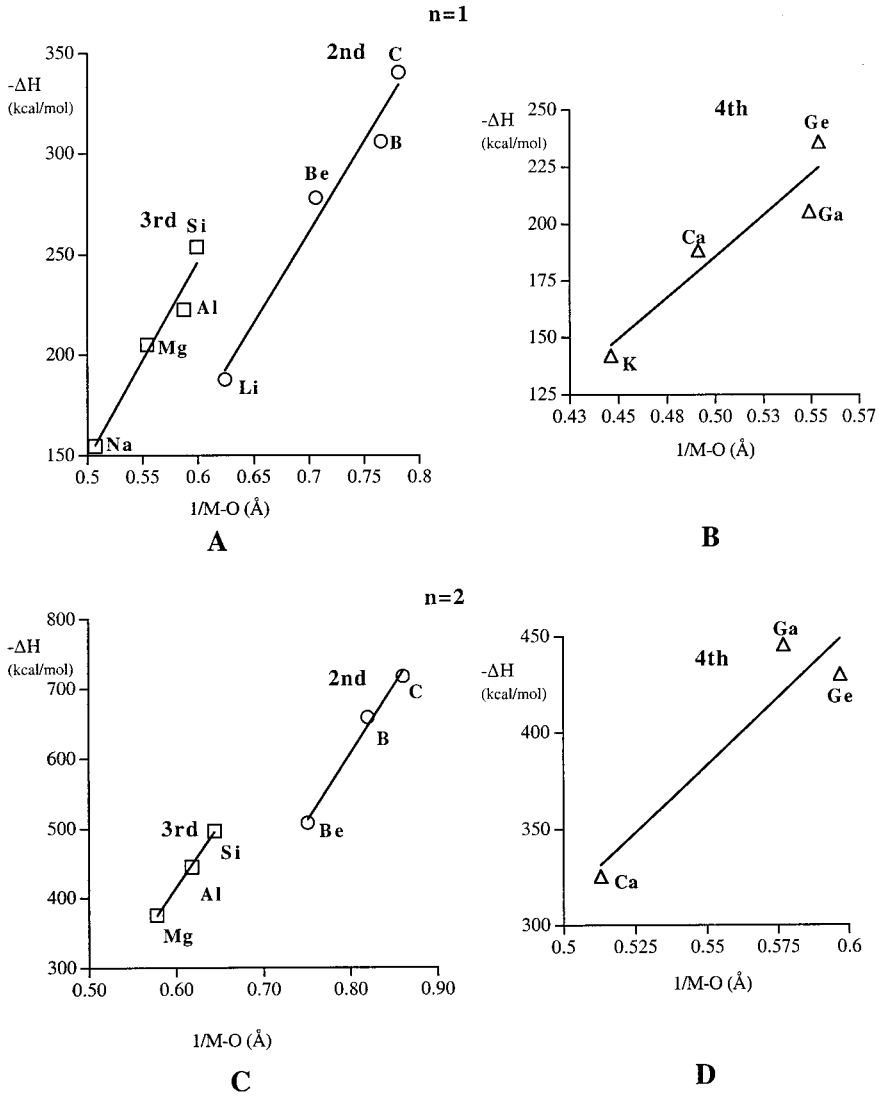

Figure 3. Plots of $-\Delta H^\circ_{298}$ versus 1/M−O for the main group metal ion monohydroxides, $M^{n+}[OH^-]$ in groups 2A, 3A, and 4A in the second, the third, and the fourth periods using energies from the CCSD(T) computational level. Thermal corrections and M−O distances (Å) were calculated at the MP2 level.

correlation coefficient is 0.86; see Table 4S of the Supporting Information. The slope of the line, −975 (kcal/mol)/Å, is much larger than that found for the corresponding hydrates, −119 (kcal/mol)/Å,[27] showing ΔH°_{298} for the hydroxides to be a much more sensitive function of the metal−oxygen distance. The inverse relationship between M−O distance and ΔH°_{298} also holds for the divalent hydroxides provided the linear structures, $Ca^{2+}[OH^-]$ to $V^{2+}[OH^-]$, and the bent structures, $Cr^{2+}[OH^-]$ to $Zn^{2+}[OH^-]$, are treated separately; see Figure 5B and Table 4S.

Since $M(OH)^+$ and $M^{2+}[OH^-]$ are but alternative structural representations for the same molecule, it is interesting to note that the dissociation energies for the formation of M^+ and the $OH^\bullet$ radical (ref 53, D_o values) are significantly smaller than those for the formation of M^{2+} and the OH^- anion (Table 1 above, ΔH°_{298} values): 118 and 371 kcal/mol for Sc, 109 and 379 kcal/mol for Ti, 96 and 386 kcal/mol for V, 65 and 422 kcal/mol for Co, 51 and 433 kcal/mol for Ni, and 28 and 446 kcal/mol for Cu. These differences arise because the electron affinities of the 2+ ions far exceed that of the $OH^\bullet$ radical. For example, in the case of Co, using data computed at the CCSD-(T) level, the difference in dissociation energies, −360 kcal/mol, is given by combining the ΔH°_{298} values for the two reactions:

$$Co(OH)^+ \rightarrow Co^+ + OH^\bullet \qquad +62$$

$$Co^{2+} + OH^- \rightarrow Co^{2+}[OH^-] \text{ (or } Co(OH)^+) \qquad -422$$

$$\text{net: } Co^{2+} + OH^- \rightarrow Co^+ + OH^\bullet \qquad -360$$

The same energy difference results from the combination of the electron affinities for Co^{2+} and the $OH^\bullet$ radical:

$$OH^- \rightarrow OH^\bullet + e^- \qquad +31$$

$$Co^{2+} + e^- \rightarrow Co^+ \qquad -391$$

$$\text{net: } Co^{2+} + OH^- \rightarrow Co^+ + OH^\bullet \qquad -360$$

For the first transition group metal ions in general the electron affinities[67]

$$M^+ + e^- \rightarrow M$$

$$M^{3+} + e^- \rightarrow M^{2+}$$

are also greater than the electron affinity of the $OH^\bullet$ radical, especially the latter, so the dissociation energies for the fission

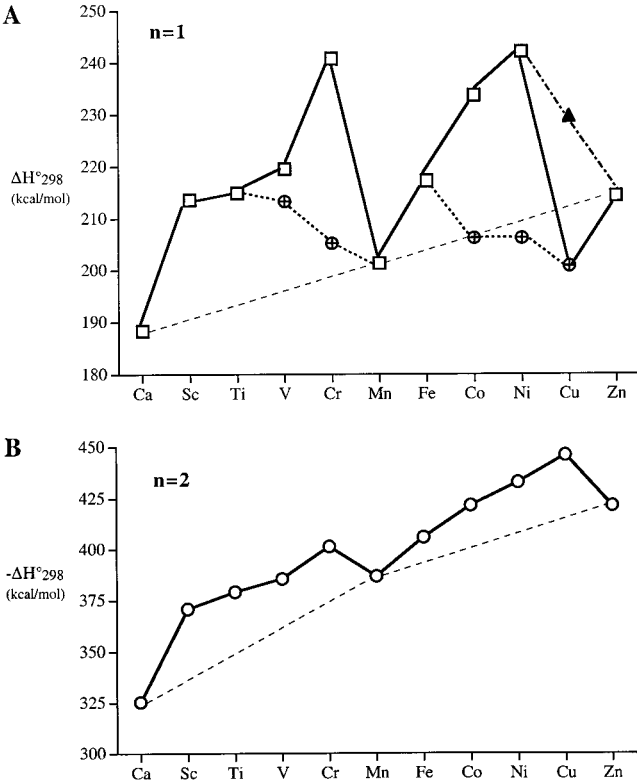

Figure 4. Variation of the enthalpy of hydration for the (A) monovalent ($n = 1$) and (B) divalent ($n = 2$) transition metal monohydroxides. (A) The points designated with □ were calculated using the lowest energy ($4s^13d^n$) state of the metal ion hydroxide $M^+[OH^-]$, and the corresponding ($4s^13d^n$) state for the isolated metal ion M^+ (which was not always the lowest energy state for this metal ion); the points designated ⊗ were calculated using both the lowest energy state of the metal hydroxide and the lowest energy state of the isolated ion (and for Cr^+, Co^+, and Ni^+ contains a significant contribution from orbital reorganization); the point designated ▲ was obtained using a triplet state of Cu^+ and $Cu^+[OH^-]$ in which the 4s orbital occupancy is nearly one; (B) The points designated with ○ were obtained from $4s^03d^n$ states for all the metal ion hydroxides, $M^{2+}[OH^-]$, and isolated metal ion, M^{2+}.

Table 4. Comparison of the Calculated Ligand Field Stabilization Energies for $M^{2+}[OH^-]$ and $M^{2+}[OH_2]$ (M = Fe, Co, Ni, and Ca) with the Experimental Values for the Hexaaquo-Ion and Values Derived from Lattice Energies of the Fluoro, Chloro, and Oxide Ions[27,69]

	ligand field stabilization energies (kcal/mol)			
bonding of M^{2+}	Fe^{2+}	Co^{2+}	Ni^{2+}	Cu^{2+}
A. calculated (CCSD(T))				
$M^{2+}[OH^-]$	12	21	25	32
$M^{2+}[OH_2]$	6	13	6	11
B. experimental				
M_{aq}^{2+}	17	24	34	25
$M^{2+}[F^-\cdot lattice]$	26	28	38	29
$M^{2+}[Cl^-\cdot lattice]$	16	25	30	28
$M^{2+}[O^{2-}\cdot lattice]$	18	23	36	32

of M(OH) and $M(OH)^{2+}$ giving the $OH^\bullet$ radical would likewise be less than the energies for the dissociation in which the OH^- anion is formed.

E. Deprotonation Enthalpies. ΔH°_{298} values for the deprotonation of $M^{n+}[OH_2]$ via *proton dissociation*, reaction 1, have been obtained by summing the calculated ΔH°_{298} values for the reactions

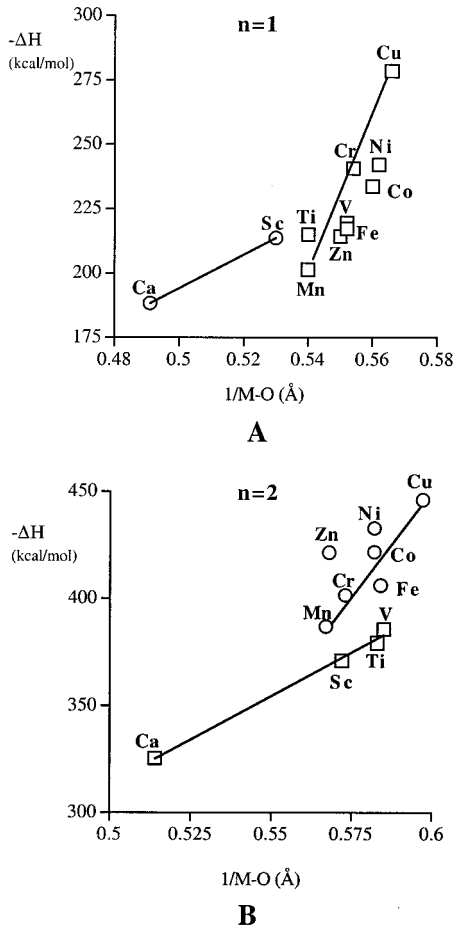

Figure 5. Plots of $-\Delta H^\circ_{298}$ versus 1/M−O for the monovalent and divalent transition metal ion monohydroxides.

$$M^{n+}[OH_2] \rightarrow M^{n+} + H_2O$$

$$H_2O \rightarrow OH^- + H^+$$

$$M^{n+} + OH^- \rightarrow M^{n+}[OH^-]$$

$$\text{net:} \quad M^{n+}[OH_2] \rightarrow M^{n+}[OH^-] + H^+ \qquad (1)$$

$$\text{i.e.} \quad \Delta H^\circ_{298}(1) = \Delta H^\circ_{298}(M^{n+}[OH^-]) + \Delta H^\circ_{298}(H_2O \rightarrow OH^- + H^+) - \Delta H^\circ_{298}(M^{n+}[OH_2])$$

and for deprotonation via *proton transfer to water*, reaction 2, by summing the calculated ΔH°_{298} values for

$$M^{n+}[OH_2] \rightarrow M^{n+} + H_2O$$

$$H_2O + H_2O \rightarrow OH^- + H_3O^+$$

$$M^{n+} + OH^- \rightarrow M^{n+}[OH^-]$$

$$\text{net:} \quad M^{n+}[OH_2] + H_2O \rightarrow M^{n+}[OH^-] + H_3O^+ \qquad (2)$$

$$\text{i.e.} \quad \Delta H^\circ_{298}(2) = \Delta H^\circ_{298}(M[OH^-]) + \Delta H^\circ_{298}(H_2O + H_2O \rightarrow OH^- + H_3O^+) - \Delta H^\circ_{298}(M^{n+}[OH_2])$$

The values of ΔH°_{298} ($H_2O \rightarrow OH^- + H^+$) and ΔH°_{298} (H_2O +

Table 5. ΔH°_{298} Values, kcal/mol, for Reactions of HO^-, H_2O, and H_3O^+ Calculated at (i) the MP2(FULL)/6-311++G**//MP2(FULL)/6-311++G** and (ii) the CCSD(T)(FULL)/6-311++G**//MP2-(FULL)/6-311++G** Computational Levels, Compared with Experimental Values

reaction	MP2	CCSD(T)	expt
$H_2O \rightarrow HO^- + H^+$	+390.6	+394.3	+390.8[a]
$H_2O + H^+ \rightarrow H_3O^+$	−165.0	−166.4	−165.8[b]
$H_2O + H_2O \rightarrow HO^- + H_3O^+$	+225.6	+227.9	+225.0

[a] Reference 70, p 781, and references cited therein. [b] Reference 71, pp 700, and 701: and references cited therein.

$H_2O \rightarrow OH^- + H_3O^+$) are in good agreement with experiment; see Table 5.[70,71]

In almost all cases, deprotonation via proton dissociation is a very unfavorable process compared to proton transfer to water. The difference is approximately 165 kcal/mol (compare Tables 6A,B with 5SA,SB, respectively); see Table 5. Although proton dissociation values can serve for purposes of comparison, these large endothermicities rule it out as the mechanism for metal ion hydroxide formation in biological systems.

The ΔH°_{298} values for deprotonation via proton transfer to H_2O, on the other hand, show a changeover from unfavorable to favorable as the charge on the ion goes from 1 to 2; see Table 6A,B. For the monovalent main group ions (except B and C) and the transition metal ions the values are again positive, ranging from +10 to +110 and from +40 to +65 kcal/mol, respectively. On the other hand, those for the divalent main group and transition metal ions range from −50 to −250 and from −50 to −115 kcal/mol, respectively.

In contrast to these very favorable energies for the deprotonation of the *mono*hydrates of the transition metal ions, previous calculations[46] found that the bonding of *six* H_2O molecules in the first coordination shell of Mn^{2+} and Zn^{2+},

$$M^{2+}[OH_2]_6 + H_2O \rightarrow M^{2+}[OH_2]_5[OH^-] + H_3O^+$$

resulted in a far smaller (but still favorable) deprotonation energy of −10.2 kcal/mol for $Zn^{2+}[OH_2]_6$, and in a positive (unfavorable) value of +2.9 kcal/mol for $Mn^{2+}[OH_2]_6$. Further calculations find the value for $Ca^{2+}[OH_2]_6$ to be +10.9 kcal/mol, even more positive than that for $Mn^{2+}[OH_2]_6$; see Table 6S, which suggests that there is a regular trend from relatively small positive to relatively small negative values across the hexahydrates of the transition series Ca^{2+} to Zn^{2+}.

The reason for this drastic reduction in the deprotonation enthalpy is not far to seek. As more water molecules pack around the metal ion in its first coordination shell, the $M^{n+}[OH_2]$ bond is weakened and the effect of the metal ion is decreased. It has already been established that there is a progressive decrease in ΔH°_{298} for the sequential bonding of one through four H_2O molecules in the first coordination shell of Be^{2+},[34] and in the bonding of one through six H_2O molecules in the first coordination shell of Mg^{2+}, Ca^{2+}, and Zn^{2+}.[43−46] Taking Mg^{2+} and its hydrates for illustrative purposes, a similar but far more pronounced decrease in ΔH°_{298} for $Mg^{2+}[OH^-]$ bonding as the number of first coordination sphere water ligands increases has been found; see Figure 6. As a consequence the difference between ΔH°_{298} for OH^- and H_2O bonding decreases as the number of additional H_2O molecules bonded to the Mg^{2+} goes from zero to five, and is of such a magnitude as

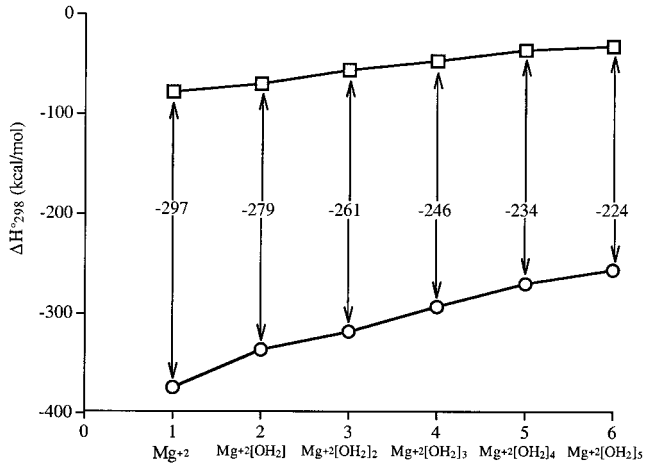

Figure 6. ΔH°_{298} for the sequential bonding of H_2O (□) and OH^- (O): 1, to Mg^{2+}; 2, to $Mg^{2+}[OH_2]$; 3, to $Mg^{2+}[OH_2]_2$; 4, to $Mg^{2+}[OH_2]_3$ calculated at the MP2 level; 5, to $Mg^{2+}[OH_2]_4$; 6, to $Mg^{2+}[OH_2]_5$ calculated at the MP2(FULL)/6-311++G**//HF/6-31G* level.

to reduce the deprotonation energy by some 70 kcal/mol in the hexahydrate.

It may be noted that H_2O is one of many bases—uncharged or anionic—that can, in principle, serve as the proton acceptor in the deprotonation of metal ion hydrates,

$$M^{2+}[OH_2] + B \rightarrow M^{2+}[OH^-] + BH^+$$

$$M^{2+}[OH_2] + B^- \rightarrow M^{2+}[OH^-] + BH$$

If the proton affinity of the base is greater than that of H_2O, 165 kcal/mol, see Table 5, then the deprotonation energy of the metal ion hydrate is more *exothermic* by the difference in the proton affinities. In enzyme systems, proton transfer to amino acid side chain groups would appear to be quite feasible in view of the proton affinities of corresponding bases. The model side chains $CH_3CH_2NH_2$ (lysine), imidazole (histidine), and indole (tryptophan) have proton affinities of 217, 223, and 188 kcal/mol, respectively; $CH_3CH_2O^-$ (serine), CH_3S^- (cysteine), $C_6H_5O^-$ (tyrosine), and $CH_3CH_2CO_2^-$ (aspartic and glutamic acids) have experimental values of 377, 357, 349, and 348 kcal/mol, respectively.[70,71] Proton transfer from the metal ion hydrate to bases with proton affinities such as these would thus more than offset the decrease of some 70 kcal/mol in deprotonation energy that arises from the bonding of multiple H_2O molecules in the first coordination shell. Since this trend is likely to be the case for any metal ion, it is unlikely to be the primary determinant of the selection for a particular metal−protein pair in a functional complex.

Discussion

In practice the ability of metal ions to facilitate the ionization of water is expressed by pK_a values for the reaction[72]

$$M_{aq}^{n+} + H_2O_{liq} \rightarrow M^{n+}OH_{aq}^- + H_{aq}^+$$

Using values from a critical compilation of experimental data,[73]

(70) Lias, S. G.; Bartmess, J. E.; Liebman, J. F.; Holmes, J. L.; Levin, R. D.; Mallard, W. G. *J. Phys. Chem. Ref. Data* **1988**, *17*, Suppl. 1.

(71) Lias, S. G.; Liebman, J. F.; Levin, R. D. *J. Phys. Chem. Ref. Data* **1984**, *13* (3).

(72) $pK_a = -\log\{g_{(M^{2+}OH^-)}[M^{2+}OH^-]\ g_{H^+}[H^+]/g_{(M^{2+})}[M^{2+}]a_{H_2O}\}$, where the activity coefficients, *g*, and the activity of water, a_{H_2O}, are equal to unity at infinite dilution. $RTpK_a$ is thus the standard free energy of ionization.

(73) Baes, C. F., Jr.; Mesmer, R. E. *The Hydrolysis of Cations;* Krieger: Malabar, FL, 1976.

Table 6. Enthalpy Changes, ΔH°_{298}, kcal/mol, for the Proton Transfer. Metal Ion Monohydrates, $M[OH_2]^{n+} + H_2O \rightarrow M[OH]^{(n-1)+} + H_3O^+$ Calculated at the MP2(FULL)/6-311++G**//MP2(FULL/6-311++G** and {CCSD(T)(FULL)/6-311++G**//MP2(FULL)/6-311++G**} Computational Levels

A. From the Main Group

n	period	group 1A	group 2A	group 3A	group 4A	n	period	group 2A	group 3A	group 4A
1	2	Li	Be	B	C	2	2	Be	B	C
		+72.6	+10.4	−29.9	−32.9			−139.4	−209.8	−258.5
		{+74.0}	{+8.1}	{−30.0 }	{−30.4 }			{−139.3}	{−212.3}	{−254.0}
	3	Na	Mg	Al	Si		3	Mg	Al	Si
		+95.0	+53.1	+30.7	+16.4			−71.4	−121.7	−154.6
		{+96.8}	{+53.8}	{+31.5}	{+16.7}			{−70.9}	{−119.8}	{−173.9}
	4	K	Ca	Ga	Ge		4	Ca	Ga	Ge
		+103.1	+65.4	+44.2	+27.1			−53.0	−122.1	−131.8
		{+105.5}	{+63.2}	{+45.6}	{+28.9}			{−48.1}	{−122.6}	{−121.5}

B. From the First Transition Series

n	group 2A M = Ca	group 3B M = Sc	group 4B M = Ti	group 5B M = V	group 6B M = Cr	group 7B M = Mn	group 8 M = Fe	group 8 M = Co	group 8 M = Ni	group 1B M = Cu	group 2B M = Zn
1	+65.4	+48.1	+49.1	+50.8	+74.7	+50.0	+48.1	+87.1	+107.7	+58.5	+44.8
	{+63.2}	{+48.7}	{+49.4}	{+50.2}	{+53.3}[a]	{+54.3}	{+43.1}	{+58.8}[a]	{+58.0}[a]	{+63.2}[a]	{+45.5}
2	−53.0	−78.0	−78.8	−79.1	−87.2	−81.8	−92.8	−94.2	−95.3	−105.3	−100.8
	{−48.1}	{−76.6}	{−80.8}	{−83.1}	{−89.2}	{−83.4}	{−91.9}	{−99.1}	{−111.5}	{−115.7}	{−99.9}

[a] Computed values using $4s3d^n$ orbital occupancy for the corresponding metal ions.

Table 7. Linear Relationships between (A) the Experimental pK_a Values[73] for Proton Dissociation from the Mg^{2+}, Ca^{2+}, Mn^{2+}, Fe^{2+}, Co^{2+}, Ni^{2+}, Cu^{2+}, and Zn^{2+} Aquo-Ions, $M^{2+}{}_{aq} + H_2O_{liq} \rightarrow M^{2+}OH^-{}_{aq} + H^+{}_{aq}$, and ΔH°_{298} Values Calculated for Related Reactions in the Gas Phase, (B) the ΔH°_{298} Values for the Gas Phase Dissociation Reaction A(iv) and the Reciprocal M−O Bond Lengths in the Monohydrates and Monohydroxides, and (C) the Experimental pK_a Values and the Reciprocal Bond Lengths

A	reaction	equation	correlation coeff
(i)	$M^{2+} + H_2O \rightarrow M^{2+}[OH_2]$	$pK_a = 17.53 + 0.0877\Delta H^\circ_{298}$(i)	$r = 0.94$
(ii)	$M^{2+} + OH^- \rightarrow M^{2+}[OH^-]$	$pK_a = 16.34 + 0.0164\Delta H^\circ_{298}$(ii)	$r = 0.87$
(iii)	$M^{2+} + H_2O \rightarrow M^{2+}[OH^-] + H^+$	$pK_a = 10.53 + 0.0487\Delta H^\circ_{298}$(iii)	$r = 0.94$
(iv)	$M^{2+}[OH_2] \rightarrow M^{2+}[OH^-] + H^+$	$pK_a = 3.43 + 0.0854\Delta H^\circ_{298}$(iv)	$r = 0.98$

B	bond length	equation	correlation coeff
(i)	$M^{2+}-OH_2$	ΔH°_{298}(iv) = 328−487 (1/M−O)	$r = -0.94$
(ii)	$M^{2+}-OH^-$	ΔH°_{298}(iv) = 409−578 (1/M−O)	$r = -0.83$

C	bond length	equation	correlation coeff
(i)	$M^{2+}-OH_2$	$pK_a = 31.13-40.99$ (1/M−O)	$r = -0.91$
(ii)	$M^{2+}-OH^-$	$pK_a = 38.30-49.31$ (1/M−O)	$r = -0.82$

Chang and Wang[74] found a linear relationship between the pK_a for $Mg_{aq}{}^{2+}$, $Ca_{aq}{}^{2+}$, $Mn_{aq}{}^{2+}$, $Zn_{aq}{}^{2+}$, $Cd_{aq}{}^{2+}$, $Al_{aq}{}^{3+}$, $Sc_{aq}{}^{3+}$, $Cr_{aq}{}^{3+}$, $Fe_{aq}{}^{3+}$, $Ga_{aq}{}^{3+}$, and $In_{aq}{}^{3+}$, and calculated binding energies for the corresponding *hexahydrates*, $M^{n+}[OH_2]_6$. The binding energy, E_b, was defined as $-(E_t - E_a)$, where E_t is the total energy of the hexahydrate ion and E_a is the sum of the energies of the component atoms. The calculations were carried out using DFT methodology (local density approximation[75]) with a numerically defined double-ζ basis set that included polarization functions on all the atoms; the DMOL.v950 program was used by them throughout.[76]

With only one water molecule bound to the divalent ions Mg^{2+}, Ca^{2+}, Mn^{2+}, Fe^{2+}, Co^{2+}, Ni^{2+}, Cu^{2+}, and Zn^{2+} we find a linear relationship between the values of ΔH°_{298}(i) for the reaction $M^{2+} + H_2O \rightarrow M^{2+}[OH_2]$ (reported in part 1[27]) and the corresponding pK_a values,

$$pK_a = 17.53 + 0.0877\Delta H^\circ_{298}(\text{i}) \qquad r = 0.94$$

Furthermore the calculated values of ΔH°_{298}(ii) from Table 1A,B for the bonding of OH^- to the same group of divalent ions give a similar linear relationship,

$$pK_a = 16.34 + 0.0164\Delta H^\circ_{298}(\text{ii}) \qquad r = 0.87$$

see Table 7A(i,ii). It is to be expected, therefore, that ΔH°_{298} for proton dissociation, either from M^{2+} and H_2O as separate entities or from the monohydrate $M^{2+}[OH_2]$, would also show a linear relationship since proton dissociation is the outcome of ΔH°_{298} for hydroxide formation exceeding that for hydrate formation. Comparison of the two sets of data shows that ΔH°_{298} for hydroxide formation is, on average, 4.5 ± 0.5 times greater than that for hydrate formation. The linear equations for these two proton dissociation reactions, with correlation coefficients of 0.94 and 0.98 respectively, are given in Table 7A(iii,iv).

The values of ΔH°_{298}(i) for the formation of the hydrate and ΔH°_{298}(ii) for the formation of the hydroxide are both linearly related to the reciprocal of the M−O bond lengths; see part 1[27] and Figure 3 above. Therefore, since ΔH°_{298}(iv) for proton dissociation has been found to be a linear function of both ΔH°_{298}(i), and ΔH°_{298}(ii), it follows that ΔH°_{298}(iv) should be a linear function of 1/M−O for the hydrate, and of 1/M−O for the hydroxide, which is borne out by the equations given in Table 6B(i,ii).

(74) Chang, C. M.; Wang, M. K. *Chem. Phys. Lett.* **1998**, *286*, 46−50.
(75) Vosko, S. H.; Wilk, L.; Nusair, M. *Canadian J. Phys.* **1980**, *58*, 1200−1211.
(76) *DMOL*, version 950; Biosym Technologies, Inc: San Diego, CA, 1995.

It is, nevertheless, somewhat surprising to find that the pK_a values are likewise a linear function of the reciprocal bond lengths; see Table 7C(i,ii). Presumably the changes in the M−O bond length in the water molecules that undergo ionization in the aquo-ions closely parallel the changes in the monohydrates. Besides electronic factors contributing to the variation of ΔH°_{298}(iv) and pK_a with 1/M−O, such as the extent of electron transfer from H_2O and OH^- to the metal ion, electrostatic interaction is clearly important. The longer the M−O distance, the less repulsion there would be between the M^{2+} ion and the H-atom that is about to dissociate as H^+, and hence the ionization would be less favored: the shorter the M−O distance, the more repulsion there would be, and the ionization would be more favored.

Further calculations are being carried out on the bonding of six water molecules to mono-, di-, and trivalent transition metal ions and on the related ionization,

$$M^{n+}[OH_2]_6 \rightarrow M^{n+}[OH_2]_5[OH^-] + H^+$$

Comparison of these data with those for the aqueous solution ionization will reveal the extent to which bonding beyond the first solvation shell contributes to the reactivity and whether there are specific features characteristic of the particular metal ion(s), notably their classification as "hard" or "soft."[77] In the case of $Zn^{2+}[OH_2]_6$, for example, it has been found that the first shell contributes only about 53% of the experimental solvation energy.[78]

Finally, we note that in order to optimize the efficiency of proton abstraction from a substrate by transfer to a metal ion hydroxide in enzymatic and nonenzymatic reactions, pK_a for the corresponding metal ion hydrate should be commensurate with pK_a for the substrate.[79] The results reported in this paper show that the ΔH°_{298} values (and hence those for pK_a) for the intrinsic ionization of the water molecule in the monohydrates span many kilocalories per mole, so, although completion of the first coordination shell by the bonding of additional water molecules or other ligands and subsequent solvation effects would modify these values, it is entirely reasonable that in aqueous solution a close match could be achieved between pK_a for the aquo-ion and pK_a for the substrate. A further consideration is the matching of the pK_a for the metal ion hydrate with pK_a for a group in the environment, so that, by proton transfer, the hydroxide is regenerated. In enzyme systems, as we have shown, proton transfer to amino acid side chain groups could well serve this purpose. While the choice of cation for a particular enzymatic role would also depend on additional factors, such as bioavailability, the intrinsic properties of the monohydrate/monohydroxide system serve as a prototype for the aqueous solution behavior.

Acknowledgment. We thank the Advanced Scientific Computing Laboratory, NCI-FCRF, for providing time on the CRAY YMP supercomputer. This work was supported by Grants CA10925 (to J.P.G.), GM31186 (to G.D.M.), and CA06927 (to Fox Chase Cancer Center (FCCC)) from the National Institutes of Health and by an appropriation from the Commonwealth of Pennsylvania (to FCCC). The authors gratefully acknowledge the technical assistance of Carol Afshar and the helpful comments of the reviewers. The contents of this paper are solely the responsibility of the authors and do not necessarily represent the official views of the National Cancer Institute.

Supporting Information Available: Tables listing the total molecular energies (au), entropies (cal/mol·K) and thermal corrections (au) for the main group and first transition group metal monohydroxides (Table 1S) (selected B3LYP/6-311++G** results are given in Table 2S), vibrational frequencies (cm^{-1}) for the main and first transition group metal ion monohydroxides (Table 3S), parameters *A* and *B* and correlation coefficients, *r*, for linear plots relating ΔH°_{298} to 1/(M−O) (Table 4S), ΔH°_{298} values (kcal/mol) for the deprotonation of the main group and first-row transition metal ion monohydrates (Table 5S), and ΔH°_{298} values (kcal/mol) for proton transfer from the bonded H_2O molecule to another H_2O molecule (Table 6S) and figures showing M−O(hydrate)−M−O(hydroxide) (Å) for the main group (Figure 1S) and first-row transition metal (Figure 2S) ions and the variation of M−O vibrational frequency (cm^{-1}) for the transition metal ion hydroxides (Figure 3S). This material is available free of charge via the Internet at http://pubs.acs.org.

IC010008P

(77) *Hard and Soft Acids and Bases*; Pearson, R. G., Ed.; Dowden, Hutchinson and Ross, Inc.: Stroudsburg, PA, 1973.
(78) Byung, J. M.; Lee, S.; Seung, J. C.; Kuntack, L.; Kim, K. S. *Chem. Phys. Lett.* **1992**, *197*, 77−80.
(79) Cleland, W. W.; Frey, P. A.; Gerlt, J. A. *J. Biol. Chem.* **1998**, *273*, 25529−25532.